Liu *et al. Human Genomics* (2025) 19:15
https://doi.org/10.1186/s40246-025-00726-9

Human Genomics

RESEARCH Open Access

The comprehensive potential of AQP1 as a tumor biomarker: evidence from kidney neoplasm cohorts, cell experiments and pan-cancer analysis

Yifan Liu[1,2†], Donghao Lyu[1†], Yuntao Yao[1,2†], Jinming Cui[3†], Jiangui Liu[1], Zikuan Bai[4], Zihui Zhao[1], Yuanan Li[1], Bingnan Lu[1*], Keqin Dong[1,5*] and Xiuwu Pan[1*]

Abstract

Aquaporin1 (AQP1) facilitates water transport. Its ability to be a biomarker at the pan-cancer level remains uninvestigated. We performed immunohistochemical staining on tissues from 370 individuals with kidney neoplasms to measure AQP1 expression. We utilized Kaplan-Meier survival analysis, Chi-square tests, and multivariate Cox regression analyses to assess the prognostic relevance of AQP1 expression. In the pan-cancer context, we explored AQP1's competing endogenous RNAs network, protein-protein interactions, genomic changes, gene set enrichment analysis (GSEA), the correlation of AQP1 expression with survival outcomes, drug sensitivity, drug molecular docking, tumor purity and immunity. AQP1 shRNA expressing 786-O cells were established. Cell proliferation was assessed by Cell Counting Kit-8 and colony formation. Transwell migration, invasion, and cell scratch assays were conducted. In our study, AQP1 expression was an independent protective factor for OS and PFS in renal cancer patients. AQP1 expression significantly correlated with survival outcomes in renal cancers, LGG, SARC, HNSC and UVM. PI-103 sensitivity was related to AQP1 expression and had potential binding cite with AQP1 protein. Knockdown of AQP1 reduced cell proliferation, migration and invasion. Our study uncovered AQP1 as a biomarker for favorable survival outcomes in renal cancers. Furthermore, the bioinformatic analysis promoted its implication in pan-cancer scope.

Keywords AQP1, Kidney neoplasm, Pan-cancer analysis, Immunohistochemistry, Biomarker

†Yifan Liu, Donghao Lyu, Yuntao Yao and Jinming Cui contributed equally to this work and all should be considered first author.

*Correspondence:
Bingnan Lu
972081060@qq.com
Keqin Dong
keqindong_0125@163.com
Xiuwu Pan
panxiuwu@126.com
[1]Department of Urology, Xinhua Hospital Affiliated to Shanghai Jiao Tong University School of Medicine, Shanghai 200092, China
[2]BGI research, BGI-Hangzhou, Hangzhou 310012, China
[3]Ulink College of Shanghai, Shanghai 201615, China
[4]Shanghai YK Pao School, Shanghai 201620, China
[5]Department of urology, Chinese PLA general hospital of central theater command, Wuhan 430061, China

Introduction

Aquaporins (AQPs) are passive H_2O transport channel proteins embedded in membranes [1]. They are prevalent in organs playing key roles in water balance, including the kidneys, eyes, brain, skin, and salivary glands. AQPs are crucial for maintaining body water balance and are essential for various cellular physiological processes that require water [2, 3]. AQP1 is the first recognized AQP, being selective for H_2O permeability [4]. The presence of AQP1 extends across multiple tissue types, encompassing kidney epithelial cells and microvascular endothelia found in organs such as the lungs [5], skeletal muscles [6], cardiac muscles [7], and the gastrointestinal system [8].

Research proved that AQP1 had the potential to serve as a screening biomarker for kidney renal clear cell carcinoma (KIRC) [9], and was correlated with the survival outcomes of KIRC and kidney renal papillary cell carcinoma (KIRP) patients [10, 11]. Additionally, several cohort studies showed that AQP1 could also serve as a prognostic biomarker in lung cancer, breast cancer (BRCA), and colon adenocarcinoma (COAD) [12–14]. AQP1 was demonstrated to be related to cancer progression by influencing tumor cell migration, angiogenesis, cell proliferation, cell-cell conjunction, and epithelial-mesenchymal transition (EMT) [15–17]. Despite these efforts, the research often focused on specific cancer types. Gaps remained in understanding the comprehensive pan-cancer potential of AQP1 as a prognostic biomarker and its ability to predict responses to selective drug treatments.

In this research, a retrospective study was conducted on 370 individuals diagnosed with kidney neoplasms at Xinhua Hospital. Immunohistochemical (IHC) staining and statistical analyses were applied to patient specimens to assess the prognostic value of AQP1 in renal cancers. Additionally, a pan-cancer study was carried out to explore the differential expression and mutation profiles of AQP1, along with its impact on patient survival, competing endogenous RNAs (ceRNAs) expression, drug sensitivity, molecular docking, tumor microenvironment, and the enrichment of specific molecular pathways. Lastly, cell experiments discovered the relationship among renal cancer cell proliferation, migration, invasion and AQP1 expression.

Methods

Patients incorporated into our study

We retrospected the information of kidney neoplasm patients who underwent therapeutic surgery at urology department of Xinhua Hospital affiliated to Shanghai Jiao Tong University School of Medicine, between 2016 and 2018. In this study, we collected surgical specimens from 370 kidney neoplasm patients. These samples included both tumor tissues and normal surgical margin tissues. During the patient enrollment process, we explicitly informed all participants that their clinical information and pathological specimens might be used for scientific research. Informed consent was obtained verbally from all participants. The follow-up data was collected until March 2021. During the staining process, 2 tumors and 67 normal slices were dislodged. Consequently, 368 tumor and 303 normal tissue slices were scored and utilized in the subsequent analyses. 71 patients were excluded because they lacked outcome information for overall survival (OS) or progression-free survival (PFS), meaning their status (alive/deceased or progression/no progression) was unavailable. Simultaneously, 4 patients were further excluded because they lacked detailed OS or PFS data (survival days or progression-free days). After these exclusions, 293 patients remained. Lastly, 10 patients were excluded for pathological outcomes not being KIRC, KIRP, or KICH. 283 patients were included in the multivariate Cox hazard regression. In our research, OS was defined as the time from the date of diagnosis to the date of death from any cause or the last follow-up. PFS was defined as the time from the date of diagnosis to the date of any documented disease progression or death, whichever occurred first.

Immunohistochemical staining

The tumor and normal tissues were fixed and embedded into tissue microarrays (TMA). The staining protocol was the same as in our previous studies, except for several slight revisions [18]. The antigen used in our cohort was AQP1 (Proteintech Cat# 20333-1-AP, RRID: AB_10666159). Antigen retrieval was done with Tris-EDTA buffer at pH 9.0. The incubation was performed at 25 °C for 1.5 h. After the staining, the TMA was scanned and scored by two urological professionals who specialized in pathology. The evaluation criteria included the level of staining intensity and the coverage of the stained region. Intensity was categorized as negative (0), weak positive [1], positive [2], and strong positive [3]. The area of staining was delineated into four categories: 0% (0), 1–10% [1], 11–40% [2], 41–70% [3], and 71–100% [4]. The intensity scores and the area scores were multiplied to obtain the overall scores for tumor and normal tissues. The contradictory score was judged by a third urological professional who specialized in pathology, leading to a convincing outcome for our data.

Statistical analyses between AQP1 expression levels and clinical variables

Based on the IHC score of AQP1, we applied "surv_cutpoint" to determine the optimal cut-off value, maximizing statistical significance. Patients were then categorized into high/low AQP1 expression groups using "surv_categorize". The functions "surv_cutpoint"

and "surv_categorize" were utilized from the R package "survmine". Using Kaplan-Meier (K-M) survival analysis and the Log-Rank test, we evaluate the survival difference between the two groups. This process was conducted separately for OS and PFS to provide a comprehensive analysis framework. Next, we performed Pearson Chi-square tests to analyze the correlation between categorical clinical variables and AQP1 expression category. Finally, we used multivariate Cox regression analysis to explore the independent predictive ability of AQP1 expression in the OS and PFS of patients. Finally, we conducted the diagnostic tests of the multivariate proportion hazard regression model.

Data sources for the bioinformatic analyses

We analyzed the transcriptomic and proteomic profiles of AQP1 in pan-cancer context using The Cancer Genome Atlas (TCGA) (https://cancergenome.nih.gov/) and the Human Protein Atlas (HPA) (https://www.proteinatlas.org/) databases [19]. We also accessed clinic al information, tumor types, estimation of stromal and immune cells in malignant tumors using expression data (ESTIMATE) score, tumor mutation burden (TMB), and microsatellite instability (MSI) from the TCGA database. Next, we used the cBioportal database to reveal the mutation pattern of AQP1 across different cancer types (https://www.cbioportal.org/). We predicted AQP1-targeted microRNAs (miRNA) by using DIANA-microT (https://dianalab.e-ce.uth.gr/microt_webserver/#/), miRWalk (http://mirwalk.umm.uni-heidelberg.de/), and miRDB (https://mirdb.org/) databases [20–22]. The miRNAs identified in all three of these databases were classified as target miRNAs. The relationship between AQP1 expression and target miRNA expression was studied through ENCORI/starbase database (https://starbase.sysu.edu.cn/) [23].

Next, we used the CellMiner (https://discover.nci.nih.gov/cellminer/home.do) and the Gene Set Cancer Analysis (GSCA) (http://bioinfo.life.hust.edu.cn/GSCA) databases to analyze the correlation between AQP1 expression and drug sensitivity [24, 25]. We downloaded the structure of AQP1 protein from Protein Data Bank (https://www.rcsb.org). We also retrieved the structure of sensitive drug from PubChem database (https://pubchem.ncbi.nlm.nih.gov/). Moreover, through the evaluation of gene expression profiles, we utilized Cell-type Identification By Estimating Relative Subsets Of RNA Transcripts (CIBERSORT) to determine the extent of immune infiltration and the fraction of different immune cell subtypes. We acquired the distribution pattern and expression levels of AQP1 in myeloid cells, T cells, and NK cells subtypes in pan-cancer scope by downloading data from single-cell RNA-seq data visualization and analysis (SCDVA) databases (http://panmyeloid.cancer-pku.cn/, http://pan-nk.cancer-pku.cn/), the ScRNA-seq Data Portal for T cell and B in Pan-Cancer database (http://cancer-pku.cn:3838/PanC_T/, http://pan-b.cancer-pku.cn/) [26–29], SC Fibroblast Atlas (http://pan-fib.cancer-pku.cn/) [30]. Lastly, we obtained the association between AQP1 expression and immune cell infiltration from the tumor immune estimation resource (TIMER) 2.0 database (http://timer.cistrome.org/) and the tumor immune dysfunction and exclusion (TIDE) database.

Data processing and analysis

The Wilcoxon rank sum test was used to analyze differences in AQP1 gene expression in patients across 33 types of cancer. Next, the patients were classified into two groups based on median AQP1 expression. The K-M survival analyses and univariate Cox regression were conducted to investigate the correlation between AQP1 expression and the OS, PFS, disease-free survival (DFS), and disease-specific survival (DSS) of patients. Then, we illustrated miRNAs and long non-coding RNAs (lncRNAs) corresponding to AQP1. ESTIMATE scores were used to evaluate the proportion of immune and stromal cells across the 33 types of cancer. The immune and stromal scores provided insights into the relationship between AQP1 and tumor purity in pan-cancer analysis [31]. Besides, we listed the drug sensitivity related to AQP1 expression. We selected drugs whose sensitivity was negatively correlated with AQP1 expression. We refined the 3D structure of AQP1 using PyMOL (Version 1.3, Schrödinger, LLC), where water molecules were removed and hydrogen atoms added. PDBQT files for both receptors and ligands were generated using AutoDock Tools [32], along with a three-dimensional grid box around the receptor binding site. AutoDock Vina was then employed to predict the optimal binding conformations between ligands and receptors, with the docking results analyzed in PyMOL [33]. The relationships among AQP1 expression, TMB and MSI were demonstrated in two radar plots. To investigate the relationship between specific immune cells infiltration and AQP1 expression in different cancers, correlation analysis was conducted on the tumor immune microenvironment (TIME). Lastly, gene set enrichment analysis (GSEA) was utilized to discover the top five signaling pathways that were associated with AQP1 expression across various cancers.

Construction of cell lines stably expressing AQP1 shRNA

We employed the human renal cell carcinoma cell line 786-O (American Type Culture Collection) in this research. We designed 3 shRNA specifically targeting AQP1, and screened the only one effective shRNA (5'-GTCTTCATCAGCATCGGTTCT-3') to suppress AQP1 expression. The other 2 shRNA were eliminated due to their poor efficiency in knocking down AQP1 expression. A scrambled shRNA sequence, 5'-TTCTCCGAACGT

GTCACGT-3', served as the control. Both shRNAs were inserted into a plasmid (hU6-MCS-CMV-Puromycin) provided by GENECHEM (Shanghai, China). The 786-O cells were then transduced with either AQP1 or control shRNA viral particles, using 5 μg/mL of HiTransG A (GENECHEM) over 48 h. Infected cells were treated with 2 μg/mL puromycin for a week to establish stable clones. Knockdown of AQP1 was validated through western blotting (WB), using a rabbit anti-AQP1 antibody at a 1:6000 dilution (#20333-1-AP, Proteintech, IL, USA).

Cell counting kit-8 (CCK-8) and colony formation assays

AQP1 knockdown 786-O cells were distributed at a density of 1000 cells per well into 96-well plates. Cell growth was analyzed using 10% CCK-8 solution, applied for 1 h. Optical density was recorded at 450 nm on days 0, 1, 2, and 3 to monitor proliferation.

For the colony formation assay, 300 cells were placed into 6-well plates. After two weeks, colonies were stained with 0.5% crystal violet and images were captured to evaluate the number of colonies formed.

Transwell and cell scratch assays

For the transwell migration assay, 10,000 AQP1 knockdown and control cells were placed in the top chambers of transwell inserts in 6-well plates, each in 100 μL of serum-free medium (RMPI 1640, #11875093, Thermo Fisher Scientific). For the transwell invasion test, the top wells were pre-coated with Matrigel (dilution 1:20; BD Biosciences, San Jose, CA, USA). Both bottom chambers of the transwell experiments were filled with RMPI 1640 containing 10% Fetal Bovine Serum (FBS) as an attractant. Following a 24-hour incubation, the cells that had migrated or invaded were harvested, then fixed with paraformaldehyde, stained with hematoxylin. The number of cells were counted by ImageJ (https://imagej.net/ij/, NIH, USA).

For the cell scratch assay, AQP1 knockdown and control cells were plated in 6-well plates at a concentration of $1*10^6$ cells per well. After 24 h, the cells formed a full monolayer. A straight scratch was made using a 20 μL pipette tip. Pictures of the scratched areas were taken right after wounding (0 h) and again 24 h later. The wound sizes were analyzed with ImageJ (NIH, USA). The wound healing area were calculated by empty area of 0 h minus empty area of 24 h, then divided the obtained result by empty area of 0 h.

Quantitative statistical analysis

Statistical analyses were carried out using R software version 4.2.2 (R Core Team (2024). _R: A Language and Environment for Statistical Computing_. R Foundation for Statistical Computing, Vienna, Austria. https://www.R-project.org/.). The data from cell experiments was analyzed using GraphPad Prism version 10.0.0 for Mac OS, GraphPad Software, Boston, Massachusetts USA, www.graphpad.com. A p-value less than 0.05 (two-tailed) was considered statistically significant. Significant factors were indicated as follows: "*" for $p<0.05$, "**" for $p<0.01$, and "***" for $p<0.001$. If the data followed a normal distribution, we used Pearson correlation and T-tests. If the data did not meet the normality assumption, we used Spearman correlation and Wilcoxon tests.

Results

The expression and prognostic effect of AQP1 in the Xinhua cohort

Our study approach was outlined in the graphic workflow (Fig. 1A). We investigated the role of AQP1 expression in the prognosis of kidney neoplasm patients from the Xinhua cohort. Beyond examining the correlation between AQP1 and renal cancer, we utilized pan-cancer databases and bioinformatic analyses to explore the role of AQP1 across multiple cancer types from genomic, proteomic, and immunological perspectives. The flowchart of inclusion and exclusion criteria and the workflow were illustrated in Figure S1**A**. The IHC staining of AQP1 was analyzed in both kidney neoplastic and normal tissues. The displayed neoplastic samples scored 0, and the displayed normal samples scored 12 (Fig. 1B). Besides, the average expression of AQP1 was significantly lower in tumor tissues than in normal tissues ($P<0.001$) (Fig. 2A). The staining scores and clinical information are categorized in Table 1 and visualized in Figure S2A. Next, the K-M survival curves and Log-Rank tests revealed that patients with AQP1 staining scores above 1 had better OS ($P<0.001$) (Fig. 2B and S2B), while those scores above 2 had better PFS ($P<0.001$) (Fig. 2C and S2C).

We used the Chi-square tests to reveal the correlation among AQP1 expression and other clinical variants. The high and low AQP1 expression groups were stratified based on a cutoff value of 1. The results were demonstrated in a heatmap (Figure S2D). Specifically, histopathological classification, T stage, stage, progression after treatment, PFS classification, and OS censor were significantly related to high or low expression of AQP1. The detailed Chi-square tests of these variants were presented in Fig. 2D. KIRC patients were more dominant in elevated AQP1 expression groups than in low groups ($P<0.001$). The T stage and stage were significantly correlated with AQP1 classification. Lower T stage or stage were more prevalent in high AQP1 expression groups than in low groups ($P<0.001$). The survival outcomes were also related to AQP1 expression groups. More patients in the high AQP1 expression groups had a lower probability of suffering progression after treatment or death compared to those in the low expression groups ($P<0.001$). Specifically, more patients a had

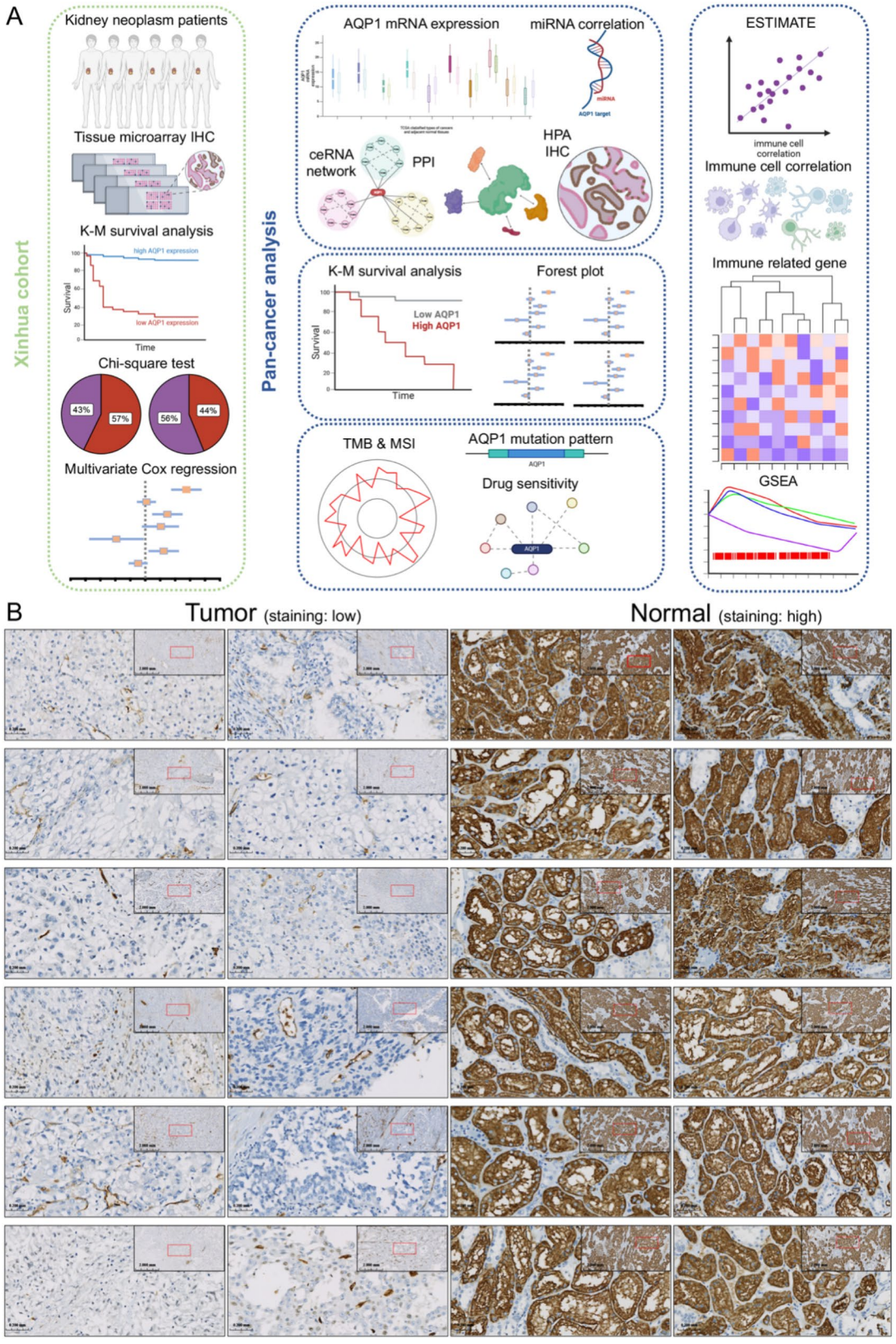

Fig. 1 (See legend on next page.)

(See figure on previous page.)

Fig. 1 The graphic workflow and IHC staing of AQP1. (**A**) The graphic workflow of our study. The left half of the figure detailed the clinical cohort aspect of our study, which encompassed AQP1 staining and subsequent analysis of its correlation with patient survival outcomes. The right half provided a visual overview of our pan-cancer research, focusing on the analysis of prognostic relationships, tumor immunity, and genomic factors. Created with BioRender.com. (**B**) 24 staining results each from tumor and normal tissues were selected and displayed. The images in the top right corner were magnified 10 times, while those in the center were magnified 40 times, providing detailed visual insights. All tumor tissues had an IHC score of 0, whereas normal tissues included IHC scored12. *IHC*, *Immunohistochemical*

higher PFS classification in high AQP1 groups than low ones ($P = 0.02$).

The independent prognostic role of AQP1 in renal cancer

We used multivariate Cox hazard regression to further analyze the role of AQP1 expression in renal cancer patients. We took age category, gender, histopathological classification, stage, and AQP1 classification tumor into analysis and generated the forest plots for the OS and PFS of renal cancer patients. High AQP1 expression independently played a protective role for OS (hazard ratio (HR) = 0.32, 95% confidence interval (CI) = 0.11–0.9, $P = 0.0308$). It also independently correlated with longer PFS (HR = 0.38, 95% CI = 0.17–0.82, $P = 0.0138$) (Fig. 2E). Based on the risk score calculated by the multivariate models, we classified the renal cancer patients into high- and low-risk groups. Besides, the high-risk groups were related to worse OS and PFS respectively (Figure S2E, F). Next, we tested the accuracy and fidelity of the multivariate model. The deviance residual plot revealed the fitting quality of the analysis. The calibration plots demonstrated the validity of the multivariate model (Figure S2F, G). Considering model diagnostics, the area under curve (AUC) of the ROC curves indicated excellent predictive outcomes. For the OS model, AUCs at 1–5 years were 0.941, 0.721, 0.777, 0.866, and 0.845, respectively. For the PFS model, AUCs at 1–5 years were 0.873, 0.824, 0.819, 0.778, and 0.744, respectively. Subsequently, the time-dependent ROC analyses revealed the excellent performance of the models at each time point (Figure S2H, I). We also generated the renal cancer patients' nomograms for OS and PFS based on the multivariate Cox regression (Figure S2G). All these analyses revealed decent accuracy, fidelity, and validity of our multivariate models.

The genomic and proteomic expression of AQP1 in pan-cancer analysis

Next, we explored the expression pattern of AQP1 in pan-cancer context. The genomic expression pattern of AQP1 among 33 kinds of cancers was demonstrated in boxplots (Fig. 3A). AQP1 expression was found to be significantly lower in bladder urothelial carcinoma (BLCA), BRCA, cervical squamous cell carcinoma (CESC), COAD, head and neck squamous cell carcinoma (HNSC), kidney chromophobe renal cell carcinoma (KICH), KIRC, lung adenocarcinoma (LUAD), lung squamous cell carcinoma (LUSC), prostate adenocarcinoma (PRAD), rectum adenocarcinoma (READ), sarcoma (SARC), and uterine corpus endometrial carcinoma (UCEC) tissues compared to their corresponding normal tissues ($P < 0.05$). On the other hand, AQP1 expression was significantly elevated in cholangiocarcinoma (CHOL), glioblastoma multiforme (GBM), and thyroid carcinoma (THCA) tissues compared to normal tissues ($P < 0.05$). In short, AQP1 expression was lower in most cancer types compared to normal tissues, except for CHOL, GBM and THCA.

We then analyzed the correlation between ceRNAs and AQP1 expression. We found 38 miRNAs that might interact with AQP1 mRNA by taking intersection of three databases (Fig. 3B). Subsequently, we demonstrated how these miRNAs were related to AQP1 expression in multiple types of cancers (Figure S3). Additionally, we investigated the lncRNAs that interacted with these 38 miRNAs. We found that 10 lncRNAs interacted with 3 of the 38 miRNAs (Fig. 3C). These 3 miRNAs were hsa-miR-1306-5p, hsa-miR-139-5p, and hsa-miR-6805-3p. The detailed relationship of each lncRNA was illustrated in Fig. 3D. Taken together, we demonstrated the ceRNAs that relevant to AQP1 expression in pan-cancer scope.

Then, we focused on the protein-protein interaction of AQP1. AQP1 protein was associated with AQP11, AQP12A, AQP7, AQP9, ANK1, EPB42, SLC4A1, RHAG, RHCE, and GYPA (Fig. 3E). RHCE and AQP1 had the strongest predicted interaction score (score = 0.924).

Finally, we collected the AQP1 IHC staining slices in the HPA database. The AQP1 expression in CHOL, renal cancer, LUAD, and LUSC showed same tendency as genomic expression (Fig. 3F). Other types of cancers' stainings were not fully aligned with the genomic expression pattern (Figure S4).

The correlation of survival outcomes and AQP1 expression in pan-cancer analysis

We further explored the prognostic implication of AQP1 with data from TCGA database ($P < 0.05$) (Fig. 4A). High expression of AQP1 was related to extended OS, PFS for KIRC, KIRP, and HNSC patients., and reduced OS, PFS for patients with low grade glioma (LGG) and uveal melanoma (UVM). The significant results of other cancers were illustataed in Figure S5.

According to the forest plots generated by univariate Cox regressions, correlations between AQP1 expression and OS, PFS, DFS, and DSS were revealed respectively (Fig. 4B). AQP1 expression was a protective factor in OS

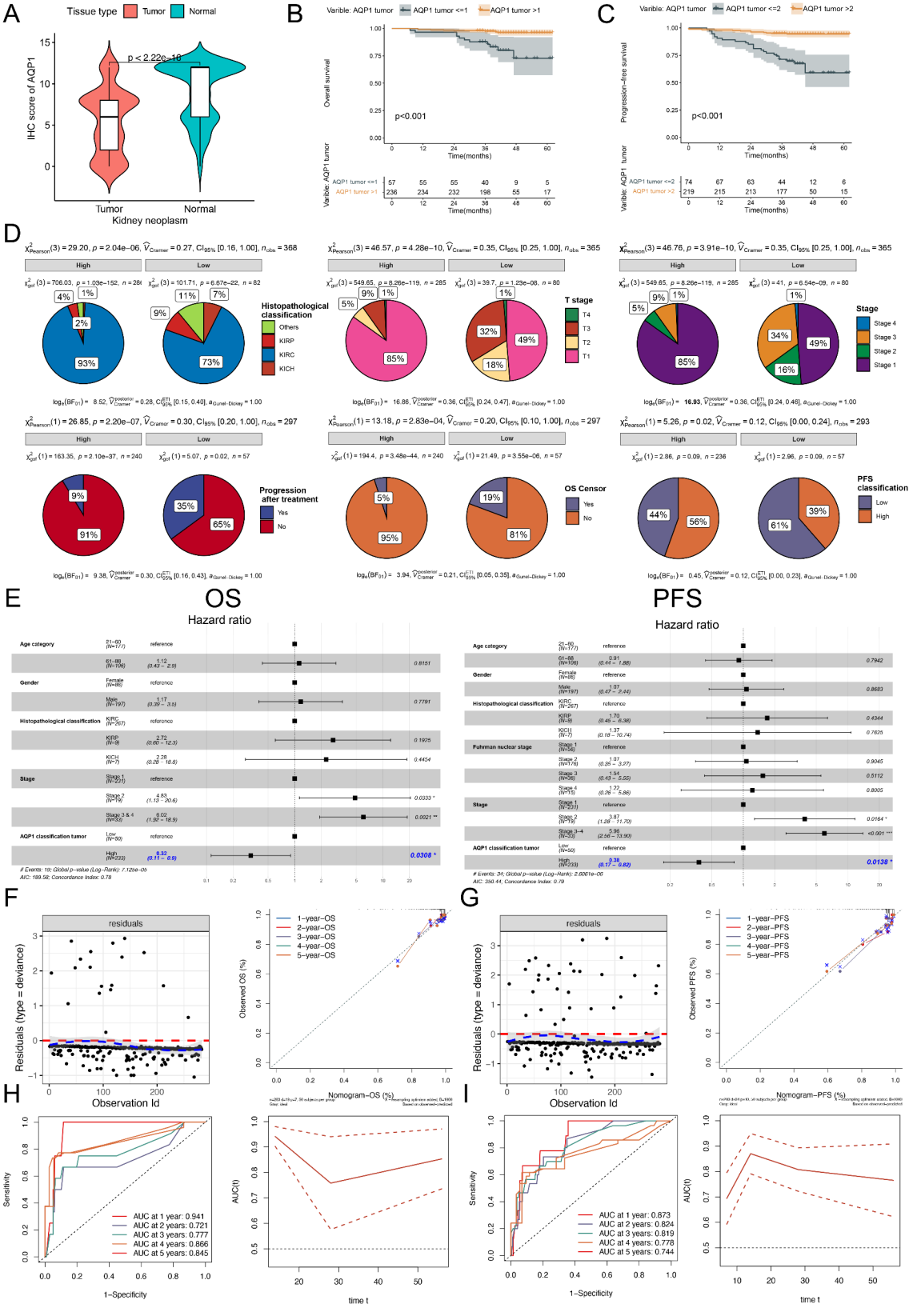

Fig. 2 (See legend on next page.)

(See figure on previous page.)

Fig. 2 Significant association between AQP1 expression and clinical variables. (**A**) The violin plot revealed the variances in AQP1 expression between neoplastic and normal tissues ($p < 0.001$). (**B**) Survival analysis using the K-M curve showed that individuals with elevated AQP1 expression in their tumor tissues had prolonged OS ($p < 0.001$). (**C**) Survival analysis using the K-M curve showed that individuals with elevated AQP1 expression in their tumor tissues had prolonged PFS ($p < 0.001$). (**D**) The analysis using Pearson's Chi-square test revealed that the presence of AQP1 in tumors was significantly linked with the classification of histopathology, T stage, stage, progression after treatment, OS censor, and PFS classification. (**E**) The forest plot showed the factors that influenced the OS and PFS of renal cancer patients. Elevated AQP1 expression in renal cancer was identified as a protective factor. *K-M, Kaplan-Meier; OS, overall survival; PFS, progression-free survival. (F-I) The model diagnosis revealed excellent accuracy and validity*

of HNSC (HR = 0.788, 95% CI = 0.683–0.910, $P = 0.001$), KIRC (HR = 0.766, 95% CI = 0.705–0.833, $P < 0.001$), KIRP (HR = 0.792, 95% CI = 0.701–0.895, $P < 0.001$), mesothelioma (MESO) (HR = 0.855, 95% CI = 0.750–0.974, $P = 0.019$), and SARC (HR = 0.845, 95% CI = 0.745–0.960, $P = 0.009$) patients. While it was a risk factor in OS of LGG (HR = 1.426, 95% CI = 1.297–1.568, $P < 0.001$), LUSC (HR = 1.104, 95% CI = 1.004–1.213, $P = 0.041$), and UVM (HR = 2.024, 95% CI = 1.295–3.165, $P = 0.002$) patients. For PFS, AQP1 expression was correlated with prolonged PFS in HNSC (HR = 0.822, 95% CI = 0.715–0.945, $P = 0.006$), KIRC (HR = 0.788, 95% CI = 0.727–0.855, $P < 0.001$), KIRP (HR = 0.849, 95% CI = 0.765–0.942, $P = 0.002$), LUAD (HR = 0.929, 95% CI = 0.867–0.996, $P = 0.037$), and SARC (HR = 0.898, 95% CI = 0.811–0.995, $P = 0.039$) patients. On the other hand, it was associated with shorter PFS in LGG (HR = 1.324, 95% CI = 1.228–1.428, $P < 0.001$) and UVM (HR = 1.818, 95% CI = 1.221–2.705, $P = 0.003$) patients. Overall, AQP1 expression was a significant protective factor in HNSC, KIRC, KIRP, and SARC patients, but a risk factor in LGG and UVM patients.

Lastly, we tested the relationship between AQP1 expression and tumors clinical stage (**Figure S6**). AQP1 expression levels in KIRC patients were lower in stage 1 than in stage 3, 4 ($P < 0.001$). In addition, in HNSC, KIRP, LIHC, and LUSC patients, stage 3 exhibited lower AQP1 expression than stage 1.

The role of AQP1 in tumor purity and therapy sensitivity in pan-cancer analysis

TMB and MSI were used to measure epigenetic changes in cancers, and they were valuable for predicting immunotherapy efficacy [34]. We analyzed the relevance between AQP1 and TMB (Fig. 5A) as well as MSI (Fig. 5B). Taken together, AQP1 expression was negatively correlated with both TMB and MSI in UCEC, stomach adenocarcinoma (STAD), skin cutaneous melanoma (SKCM), LUSC, HNSC, and BLCA patients.

Focusing on the putative copy-number alteration (CNA) of AQP1, "Gain" and "Diploid" were the most frequently identified categories in our analysis (Fig. 5C). Notably, amplification and mutations in AQP1 were prevalent across a variety of cancer types (Fig. 5D). Subsequently, we revealed that most of the mutations were missense mutations. (Fig. 5E).

We also analyzed the relationship between survival difference and AQP1 mutant/wild type, methylation, copy number variants (CNV), gene set mutation in pan-cancer scope (Figure S7). It could be summarized that in KIRC, survival outcomes were positively linked with AQP1 methylation and CNV groups. In LGG, AQP1 methylation was negatively linked with survival outcomes, while AQP1 CNV was positively linked with them.

Next, we found that AQP1 expression was significantly correlated with immune and stromal abundance across 18 cancers ($P < 0.05$) (Figure S8). We described the correlation value and p value of each cancer in Supplementary materials.

We then analyzed the relationship between drug sensitivity and AQP1 expression. CellMiner database offered perspective on AQP1 expression and drug sensitivity. We selected nine most significant drugs and demonstrated their correlation in Fig. 5F-G. The sensitivity of E-7820 ($R = 0.377$, $P = 0.003$), pentostatin ($R = 0.373$, $P = 0.003$), SNS-314 ($R = 0.310$, $P = 0.016$), mitotane ($R = 0.296$, $P = 0.022$), H-89 ($R = 0.274$, $P = 0.034$), and acetylcysteine ($R = 0.274$, $P = 0.034$) were positively linked with AQP1 expression. On the contrary, cordycepin (R = -0.291, $P = 0.024$), CT-32,228 (R = -0.277, $P = 0.032$), PI-103 (R = -0.277, $P = 0.032$) (Fig. 5G).

In CTRP database, the IC50 (half maximal inhibitory concentration) of CHIR-99,021, methylstat, ML320, NVP-TAE684, RITA, and trametinib was negatively correlated with AQP1 mRNA expression. (Fig. 5H). Other drugs related to AQP1 expression were demonstrated in Figure S9A. Similarly, the IC50 of cetuximab, PHA-665,752, SB 216,763 was negatively linked with AQP1 mRNA expression based on the data from GDSC database (Fig. 5I). Other drugs linked with AQP1 expression were demonstrated in Figure S9B.

Finally, we identified drugs whose sensitivity was nagetively correlated with AQP1 expression. Among these, PI-103 showed potential for binding to the AQP1 protein. The predicted binding site with the highest affinity was located at ASN-49, with a binding energy of -8.4 kcal/mol (Fig. 5J). Other predicted binding sites were illustrated in Figure S9C.

The correlation between immune cell infiltration and AQP1 expression

The abundence of immune cells within tumors influenced the outcome of immunotherapy [35]. In KIRC patients,

Table 1 Demographic information and clinical characteristics of the 370 patients

Variables	Number (%)	Mean ± SD; Median (range)	*P* value
AQP1 tumor	77 (20.92)	5.46 ± 3.90; 6 (0–12)	
0	5 (1.36)		
1	23 (2.73)		
2	16 (4.35)		
3	46 (12.5)		
4	29 (7.88)		
6	125 (33.97)		
8	4 (1.09)		
9	43 (11.68)		
12			
AQP1 classification tumor			
Unknown	2 (0.54)		
Low	82 (22.16)		
High	286 (72.43)		
AQP1 normal	6 (1.98)	8.95 ± 3.56; 12 (0–12)	
0	1 (0.33)		
1	5 (1.65)		
2	16 (5.28)		
3	19 (6.27)		
4	63 (20.79)		
6	9 (2.97)		
8	27 (8.91)		
9	157 (51.82)		
12			
AQP1 classification normal			0.913
Unknown	67 (18.11)		
Low	7 (18.92)		
High	296 (80.00)		
OS censor			< 0.001*
Alive	276 (92.31)		
Dead	23 (7.69)		
Unknown	71 (19.19)		
OS		42.24 ± 9.34; 41 (7–62)	
OS classification (months)			0.096
High	161 (43.51)		
Low	134 (36.21)		
Unknown	75 (20.27)		
PFS		40.99 ± 10.95; 41 (0–62)	
PFS classification (months)			0.032*
High	154 (41.62)		
Low	141 (38.10)		
Unknown	75 (20.27)		
Age (category)		56.61 ± 12.47; 55 (21–88)	0.267
21–40	33 (8.92)		
41–60	194 (52.43)		
61–88	143 (38.65)		
Gender			0.931
Female	114 (30.81)		
Male	256 (69.19)		
KIRC			< 0.001*
Yes	328 (88.65)		
No	41 (11.08)		
Histopathological classification			< 0.001*
KIRC	328 (88.65)		
KIRP	18 (4.86)		
KICH	8 (2.16)		

Table 1 (continued)

Variables	Number (%)	Mean ± SD; Median (range)	*P* value
Others	16 (4.32)		
Fuhrman nuclear stage			0.007*
Stage 1	69 (18.65)		
Stage 2	234 (63.24)		
Stage 3	51 (13.78)		
Stage 4	16 (4.32)		
T stage score		2.12 ± 1.54; 2 (1–8)	< 0.001*
T stage			< 0.001*
T1	282 (76.22)		
T2	29 (7.84)		
T3	53 (14.32)		
T4	3 (0.81)		
Unknown	3 (0.81)		
Detailed T stage			< 0.001*
1a	178 (48.11)		
1b	104 (28.11)		
2a	17 (4.59)		
2b	12 (3.24)		
3a	49 (13.24)		
3b	2 (0.54)		
3c	2 (0.54)		
4	3 (0.81)		
Unknown	3 (0.81)		
N stage			
Yes	2 (0.54)		
No	368 (11.08)		
M stage			
Yes	0 (0.00)		
No	370 (100.00)		
Stage			< 0.001*
Stage 1	282 (76.22)		
Stage 2	28 (7.84)		
Stage 3	54 (14.59)		
Stage 4	3 (0.81)		
Unknown	3 (0.81)		
Progression after treatment			< 0.001*
Yes	42 (11.35)		
No	257 (69.45)		
Unknown	71 (19.19)		

Abbreviations: SD, standard deviation; OS, overall survival; PFS, progression-free survival; KIRC, kidney renal clear cell carcinoma; KIRP, kidney renal papillary cell carcinoma; KICH, kidney chromophobe renal cell carcinoma. For variables with a p value less than 0.05 in the Chi-square tests, a "*" was assigned

resting mast cells ($R = 0.27$), monocytes ($R = 0.17$), and NK cell resting ($R = 0.15$) were positively linked with AQP1 expression ($P < 0.001$). On the contrary, macrophage M0 (R = -0.27) and Tregs (R = -0.19) were negatively linked with AQP1 expression ($P < 0.001$). In KIRP patients, memory B cells ($R = 0.24$) and macrophage M2 ($R = 0.25$) were positively linked with AQP1 expression, while naive B cells ($R = -0.3$) and macrophage M1 ($R = -0.26$) were negatively correlated with AQP1 expression ($P < 0.001$) (Fig. 6A).

The relationship between immune cell infiltration and AQP1 expression in other types of cancer was demonstrated in Figure S10. In HNSC patients, monocytes, resting mast cells, macrophage M2, plasma cells and naïve B cells were positively related to AQP1 expression. Resting NK cells, activated mast cells, activated dendritic cells and macrophage Mo were negatively related to AQP1 expression. In SARC patients, naïve B cells and resting mast cells were positively correlated with AQP1 expression.

We used the TIMER2.0 database to illustrate the correlation analysis between immune cell infiltration and AQP1 expression across pan-cancer scope (Figure S11). In UVM, the infiltration of CD8 + T cells was significantly

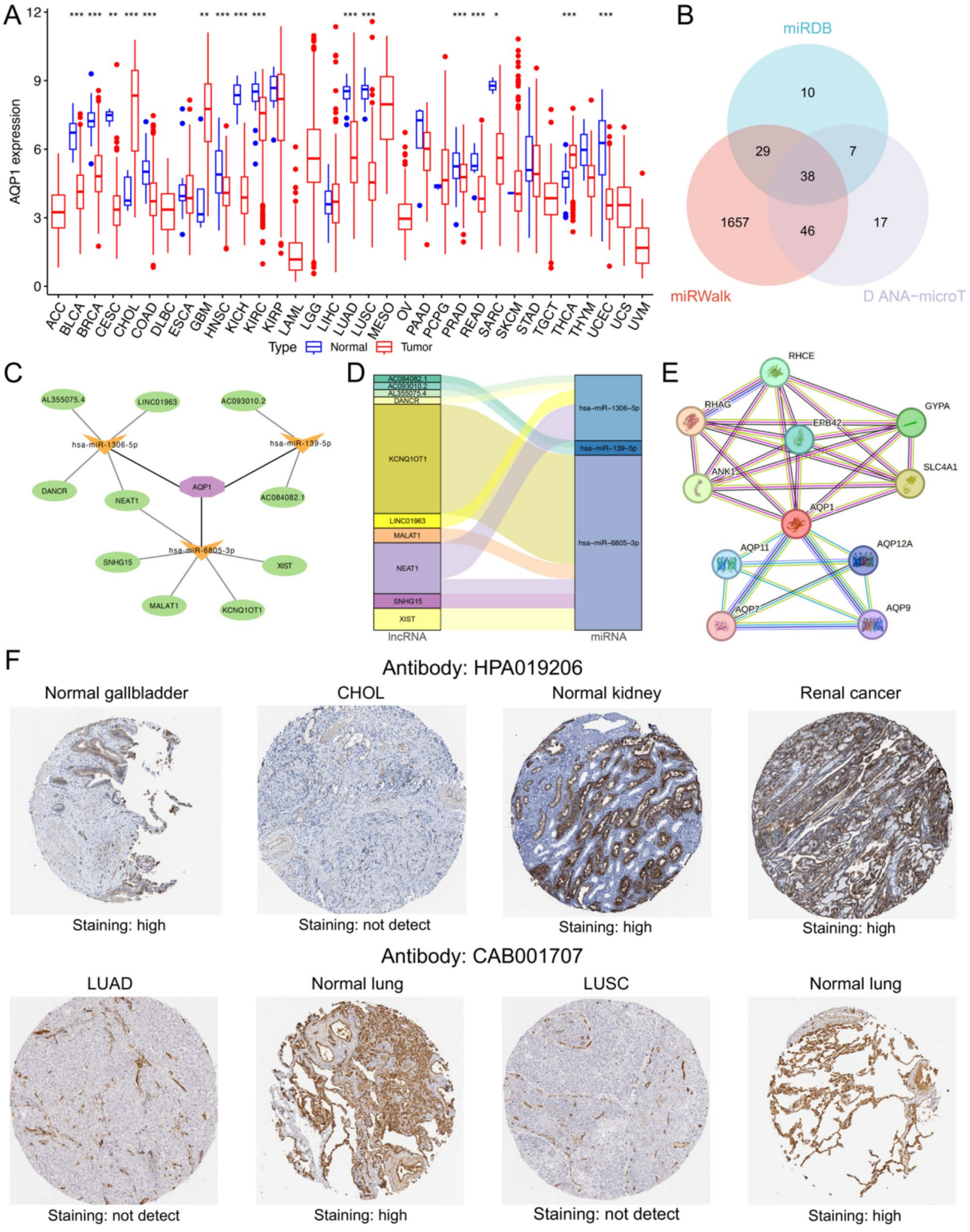

Fig. 3 (See legend on next page.)

(See figure on previous page.)

Fig. 3 Differential Expression and ceRNAs of AQP1 in Pan-Cancer context. (**A**) Differences in AQP1 expression between tumor and normal tissues according to the TCGA database. (**B**) The miRNAs predicted by three miRNA database, only 38 miRNAs were intersected by all three database. (**C**) AQP1 with its ceRNAs. Yellow triangles were miRNAs and green nodes were lncRNAs. (**D**) Sankey plot demonstrated the relationship of miRNAs and lncRNAs. (**E**) The protein network showed the proteins that coexpressed or co-effected with AQP1. (**F**) The IHC stainings of HNSC, THCA, CESC, COAD, renal cancers, UCEC, and corresponding normal tissue from the HPA database. Staining scores were consistent with the TCGA database. *miRNA, microRNA; ceRNA, competitive endogenous RNA; lncRNA, long noncoding RNA; HNSC, head and neck squamous cell carcinoma; THCA, thyroid carcinoma; CESC, cervical squamous cell carcinoma; COAD, colon adenocarcinoma; UCEC, uterine corpus endometrial carcinoma*

linked to AQP1 expression, whereas in KIRP and THYM, the correlation was opposite. The infiltration of Tregs was correlated with AQP1 expression in HNSC, while it was negative in KIRC and KIRP. The other results were described in Supplementary materials.

From single-cell RNA sequencing analysis, it was demonstrated that AQP1 expression in NK cells was scattered. The highest average expression of AQP1 was in CD56dimCD16hi-c3-NFKBIA + cells (Figure S12A). AQP1 expression in B cells was also demonstrated. The highest average expression of AQP1 was in c13_Bgz_dz-like B cells (Figure S12B). AQP1 expression patterns in fibroblast cells adjacent to pan-cancer tissues were revealed in Figure S12C. AQP1 expressed predominantly in the fibroblast cells around synovium tissues.

Finally, we focused on AQP1 expression and cytotoxic T lymphocytes (CTLs) (Figure S13A). The correlation coefficient in OV, HNSC, GBM, LUAD was $r = 0.265$, 0.093, 0.29, and 0.328, respectively ($P < 0.001$). Subsequently, we explored the impact of CTL infiltration and AQP1 expression on survival probabilities across diverse tumor types. Delineating the patients into CTL top and bottom groups, the survival outcomes were significantly correlated with AQP1 expression in BRCA ($z = 3.15$, $P < 0.01$) and HNSC ($z = 3.18$, $P < 0.01$) (Figure S13B). Consequently, we illustrated that tumor samples with high AQP1 expression were enriched in dysfunctional T cells in BRCA and HNSC.

The correlation of immune-related genes (IRGs) and AQP1 expression

Besides, we discovered how AQP1 was co-expressed with IRGs in pan-caner analysis (Fig. 6B). The relationship between AQP1 and IRGs expression varied among cancer types. The co-expression of AQP1 with IRGs was associated with the type of cancer. In HNSC, LGG and UVM, most IRGs were negatively linked with AQP1 expression ($P < 0.05$). While in KIRC, half of the significant related IRGs showed a positive relationship with AQP1 expression ($P < 0.05$).

Gene set enrichment analysis of AQP1

We emphasized the pathways of tumors whose survival outcomes were related to AQP1 expression (Fig. 6C). The enriched pathways in HNSC included arrhythmogenic right ventricular cardiomyopathy, calcium signaling pathway, cardiac muscle contraction, dilated cardiomyopathy, hypertrophic cardiomyopathy (HCM). The enriched pathways in LGG included ascorbate and aldarate metabolism, autoimmune thyroid disease, pentose and glucuronate interconversation, porphyrin and chlorophyll metabolism, and regulation of autophagy. The enriched pathways in UVM included ascorbate and aldarate metabolism, autoimmune thyroid disease, pentose and glucuronate interconversation, porphyrin and chlorophyll metabolism, and regulation of autophagy. We also demonstrated the enriched pathways of other cancers in Figure S14.

Knockdown of AQP1 in 786-O cells suppressed cell proliferation, migration and invasion

Next, we examined the role of AQP1 in kidney cancer cells 786-O. A stable AQP1 shRNA-expressing cell line was generated. WB showed reduced AQP1 levels in knockdown cells versus control cells (Fig. 7A). The CCK-8 assay indicated that inhibiting AQP1 in renal carcinoma cells significantly reduced proliferation after 72 h ($P < 0.0001$, Fig. 7B). In the colony formation test, AQP1 knockdown cells developed fewer colonies than control cells ($P = 0.0041$, Fig. 7C). Additionally, transwell assays demonstrated that suppressing AQP1 impaired the migration and invasion abilities of renal carcinoma cells ($P = 0.0455$, 0.0347, Fig. 7D-E). The cell scratch test results, shown in Fig. 7F, revealed that AQP1 knockdown cells showed much slower wound closure than the control group 24 h after scratching ($P = 0.0203$).

Discussion

Overview of AQPs

AQPs are a kind of hydrophobic protein embedded in cellular membranes, existing in every living organism [1]. These proteins are characterized by channels that facilitate the regulation of water flow in and out of cells. Furthermore, these channels assist in the transport of small molecules, including anions, urea, and glycerol [3]. AQP1 is highly expressed in the proximal tubule, the descending segments of Henle's loop, and the vasa recta [4]. It is crucial for urine concentration under normal physiological conditions [3].

AQP1 was an independent favorable factor for kidney neoplasm patients

According to our cohort, AQP1 was expressed more strongly in normal kidney tissues than in kidney tumor

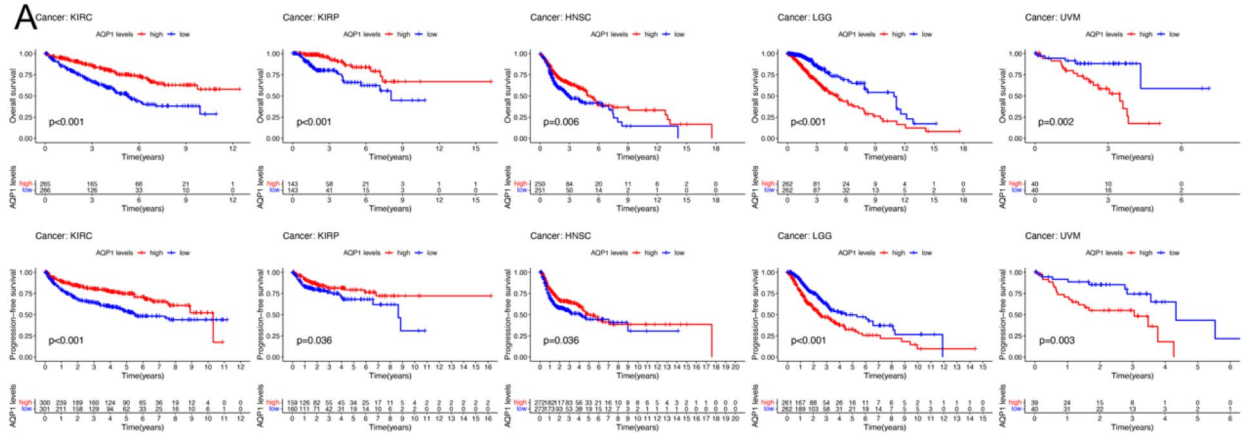

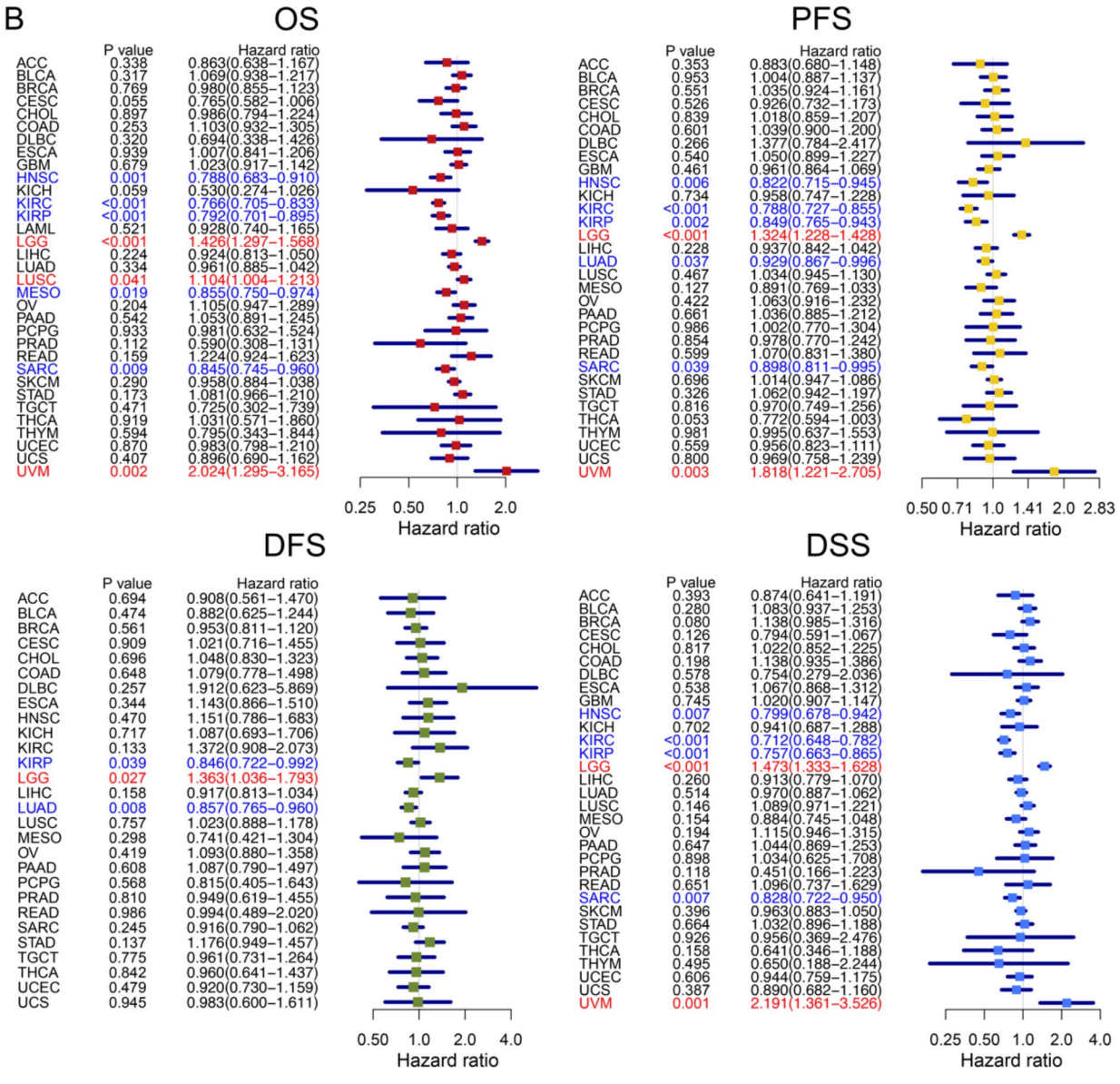

Fig. 4 (See legend on next page.)

(See figure on previous page.)

Fig. 4 Univariate analyses of survival outcomes in KIRC and pan-cancer context. (**A**) The K-M survival analysis of KIRC, KIRP, HNSC, LGG, UVM showed the correlation of AQP1 expression and OS, PFS. (**B**) Forest plot displayed the HR and 95% CI for the association of AQP1 expression with OS, PFS, DSS, and DFS in pan-cancer. Cancers where AQP1 levels showed a significant negative correlation with survival outcomes were highlighted in red. Conversely, cancers with significant positive correlations between AQP1 levels and survival outcomes were highlighted in blue. *K-M survival analysis*, *Kaplan-Meier survival analysis; KIRC*, *kidney renal clear cell carcinoma; KIRP*, *kidney renal papillary cell carcinoma; HR*, *hazard ratio; 95% CI*, *95% confidence interval*

tissues. This outcome consisted of the genomic and proteomic expression profiles of AQP1 in KIRC from TCGA and HPA databases [36]. Furthermore, AQP1 expression was an independent favorable factor for both OS (HR = 0.32, 95% CI = 0.11–0.9, $P = 0.0308$) and PFS (HR = 0.38, 95% CI = 0.17–0.82, $P = 0.0138$) of renal cancer patients. This conclusion was consistent with the results of Ying Huang et al. and David TV et al. [10, 37]. Interestingly, Ying Huang et al. analyzed the AQP1 expression through real-time quantitative reverse-transcription polymerase chain reaction. The research done by David TV et al. utilized western blot to analyze the AQP1 expression. Their work substantiated the conclusion in real-world cohorts through both genomic and proteomic analyses. Our cohort utilized IHC staining to analyze both the intensity and localization of AQP1 expression. In normal renal tissues, AQP1 was predominantly expressed in the luminal areas. However, in malignant renal tissues, AQP1 expression was scattered and lacked the organized structure observed in normal tissues. In kidney development, AQP1 was expressed at the 12th week of human nephrogenesis, marking the period when stem cells start differentiating into mature kidney cells [38]. Additionally, AQP1 was shown to be more prominently expressed in well-differentiated lung cancer tissues compared to poorly differentiated ones [39]. Together with our results, AQP1 expression levels had the potential to become a differential marker of renal cancers.

The role of AQP1 in indicating survival outcomes at pan-cancer levels

We demonstrated that AQP1 expression was lower in most types of cancer, except for CHOL, GBM and THCA. Previous studies also found that more AQP1 expression was upregulated in CHOL than normal bile duct [40, 41]. AQP1 expression was related with worse prognosis in extrahepatic CHOL [41]. In GBM, research showed that AQP1 was specifically expressed in GBM cells and facilitated tumor malignancy by promoting cell migration and invasion [42]. CHOL was highly malignant, with invasion and metastasis being very common [43]. GBM tended to exhibit dissemination [44], while THCA was often associated with early lymph node metastasis [45]. These characteristics might be related to their high expression of AQP1. In fact, cell migration and invasion require the establishment of polarity, which involves the polarized expression of ion channels in the direction of cell movement [46]. This polarization leads to changes in osmotic pressure inside and outside the cell, driving the transmembrane flow of water molecules. The high expression of AQP1 may explain the early metastatic or disseminative features of these three types of tumors.

We discovered that AQP1 expression was associated with hsa-miR-1306-5p, hsa-miR-139-5p, and hsa-miR-6805-3p using pan-cancer databases from miRWalk, miRDB, miRcode, and starbase. Our correlation analysis suggested that these miRNAs might be involved in the regulation of AQP1 expression. However, the interactions of these miRNA with AQP1 remained unclear.

Apart from renal cancers, we found that AQP1 expression was a protective factor in HNSC and SARC patients, while it was a risk factor in LGG and UVM patients. Corroborating our findings, AQP1 expression was elevated in laryngeal tumor tissues compared to nearby normal tissues [47]. AQP1 was identified as a marker for a particularly aggressive subgroup of HNSC [48]. Additionally, in a prognostic model of pyroptosis-associated genes, AQP1 expression was identified as a protective factor linked to reduced HNSC growth [49]. Besides, AQP1 was overexpressed in gliomas compared to normal brain samples, and was a risk factor for LGG patients' OS [50]. However, several studies revealed that AQP1 expression was elevated with the tumorigenesis and metastasis of osteosarcoma, which was not fully aligned with our results [51, 52].

These findings revealed the complex role of AQP1 in different cancer types, suggesting that its prognostic significance depended on the tumor context.

AQP1 and cancer treatment

We found that AQP1 expression was positively related to both immunal and stromal scores in LGG and several cancers, which indicated that higher AQP1 expression was related to lower tumor purity [31]. Besides, TMB and MSI were both negatively correlated with AQP1 expression in BLCA, UCEC, STAD, SKCM, PAAD, LUSC and HNSC. And AQP1 expression was positively related to MSI in LGG, KIRP, and THYM. Studies showed that low tumor purity was associated with better responses to immunotherapy [53]. Additionally, high TMB and MSI were both predictive of more favorable outcomes with immunotherapy [54]. Taking our results of tumor purity, TMB, and MSI together, we found that AQP1 had the potential to become a favorable biomarker of immunotherapy efficacy in LGG.

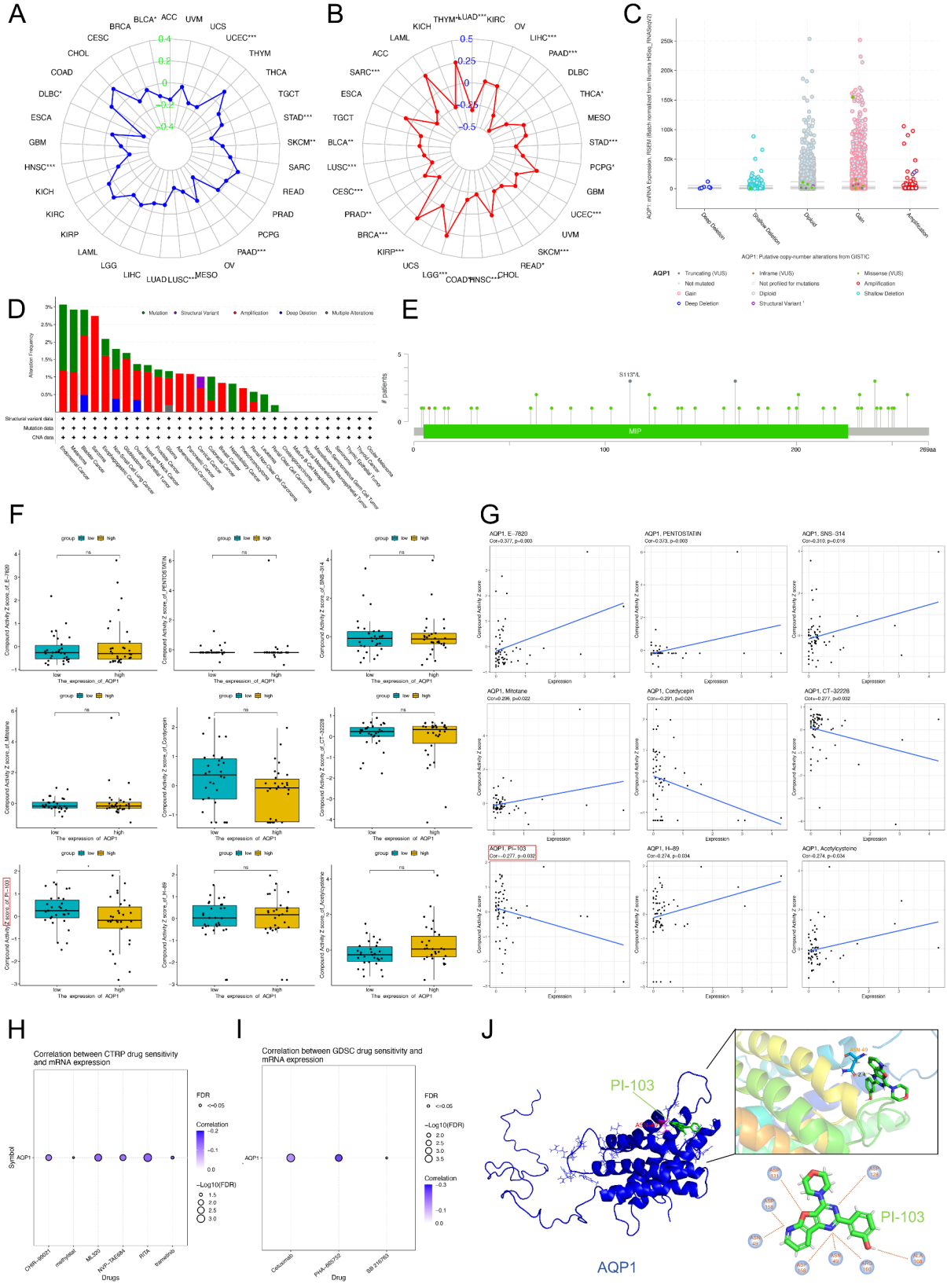

Fig. 5 (See legend on next page.)

(See figure on previous page.)

Fig. 5 The AQP1 expression correlated TMB, MSI, genomic changes and drug sensitivity in pan-cancer analysis. (**A**) Radar chart illustrated the correlation between TMB and AQP1 expression across various cancer types. Each spoke of the radar represented a different type of cancer. The distance from the center indicated the strength and direction of the correlation
outward represented a positive correlation, and inward indicated a negative correlation. Asterisks next to cancer types denoted statistical significance. AQP1 expression was negatively linked with TMB in UCEC, stomach adenocarcinoma (STAD), skin cutaneous melanoma (SKCM), pancreatic adenocarcinoma (PAAD), LUSC, HNSC, diffuse large B-cell lymphoma (DLBC), BLCA patients. (**B**) This radar chart illustrated the correlation between MSI and AQP1 expression across various cancer types. The blue line traces the correlation values for each cancer type, creating a profile of how AQP1 expression correlated with MSI across the pan-cancer analysis. AQP1 level was positively linked with MSI in LGG, KIRP, and THYM patients. It was negatively correlated in LUAD, LIHC, PAAD, THCA, STAD, PCPG, UCEC, SKCM, READ, HNSC, COAD, PRAD, CESC, LUSC, BLCA, and SARC patients. (**C**) The copy number alterations of AQP1. (**D**) The alteration frequency of AQP1 across various cancer types. (**E**) The mutation types of AQP1 in pan-cancer context. (**F**-**G**) The nine drugs whose sensitivity related to AQP1 expression predicted by CellMiner database. (**H**) The correlation between CTRP drugs and AQP1 mRNA expression. (**I**) The drugs whose sensitivity related to AQP1 mRNA expression predicted by CTRP. (**J**) The molecular docking analysis of AQP1 and PI-103. *TMB*, *tumor mutation burden; MSI*, *microsatellite instability*

Specifically, we found that the sensitivity of PI-103 was negatively correlated with AQP1 expression. Since AQP1 expressed less in renal cancers than normal tissues, PI-103 had the potential to eliminate cancer cells. PI-103 was a PI3K/mTOR inhibitor, and could inhibit hepatocellular carcinoma cell proliferation [55]. We further found that AQP1 had potential binding cite with PI-103. AQP1 could serve as a potential biomarker for predicting renal cancer patients' response to PI-103 treatment. The interaction between AQP1 and PI-103 opens up the possibility of targeting AQP1 as part of combination therapy with PI-103. Additionally, miR-133a-3p was demonstrated to suppress cell proliferation, migration and invasion via targeting AQP1 in colorectal cancer [56]. Through drug sensitivity prediction analyses and existing research, AQP1 showed its potential as a biomarker for PI-103 and miR-133a-3p in cancer treatment.

The molecular mechanisms of AQP1 in cancer

We found that AQP1 expression was correlated with the enrichment of CAMs pathway in most cancers. CAMs are proteins located on the cell membrane, primarily mediating interactions between cells or extracellular matrixs [57]. In cancer, abnormal expression and function of CAMs can promote tumor cell migration and proliferation [58].

AQP1 played a crucial role in cancer cell migration and metastasis [59]. Our experiments in renal cancer cells proved that knockdown of AQP1 suppressed cell migration and invasion. Overexpression of AQP1 in B16F10 melanoma cells, 4T1 mammary gland tumor cells, and BRCA MDA-MB-231 cells resulted in increased cell migration and invasion [60]. In non-cancerous Madin–Darby canine kidney cells, AQP1 expression didn't significantly affect cell migration [61]. Furthermore, the increased migration capability of these cancer cells correlated with a higher rate of extravasation and metastasis in vivo [59]. The correlation between AQP1 expression and CAMs pathway enrichment in cancers could be one of the mechanisms. In addition to the observed correlation, several studies had demonstrated that AQP1 contributed to cell migration through hypoxic environments and the interaction of Lin-7 with beta-catenin in neuroblastoma and melanoma [15, 62, 63].

AQP1 induced the cell proliferation in cancers. We found that knockout AQP1 in renal cancer cells resulted in inhibition of cell proliferation. In a lung cancer study, AQP1 expression was correlated with NHI-3T3 cell proliferation and anchorage-independent growth [39]. Another study showed impaired tumor growth in AQP1-null mice [64]. Overexpressing AQP1 promoted growth and colony formation in breast cancer lines MDA-MB-231 and MCF7, and enhanced proliferation in MDA-MB-231 and 4T1 cells [60, 65]. In contrast, inhibiting AQP1 expression reduced proliferation in MDA-MB-231 breast cancer cells, BALB/c nude mice, and gastric cancer cells [66, 67].

AQP1 contributed to the angiogenesis of cancers [3]. AQP1 expression was associated with micro-vessels of multiple myeloma patients [68]. Another study showed a link between AQP1 expression and VEGF levels in endometrial cancer [69]. In vivo studies of AQP1-null mice subcutaneously injected with melanoma cells also reported similar results [64]. It was indicated that the suppression of AQP1 via miRNA in the chorioallantoic membrane of chick embryos significantly inhibited blood vessel formation [70].

Based on the aforementioned literature and our results in renal cancer cell lines, we found that AQP1 played a crucial role in tumor cell proliferation, migration, and invasion. This perspective supported our findings of upregulated AQP1 expression in CHOL, GBM, THCA, and other tumors. It also explained why AQP1 served as an independent risk factor for poor prognosis in LGG and UVM. However, we observed that AQP1 expression was relatively low in KIRC, KIRP, HNSC, and SARC, where it is an independent predictor of favorable prognosis. In the context of renal cancer, AQP1 was primarily expressed in well-differentiated renal tubular epithelial cells [71, 72]. The lower expression of AQP1 in renal cancer might indicate a shift towards a less differentiated, more malignant phenotype, which could potentially correlate with poorer prognosis. While we did not have direct evidence to confirm this hypothesis, it explained

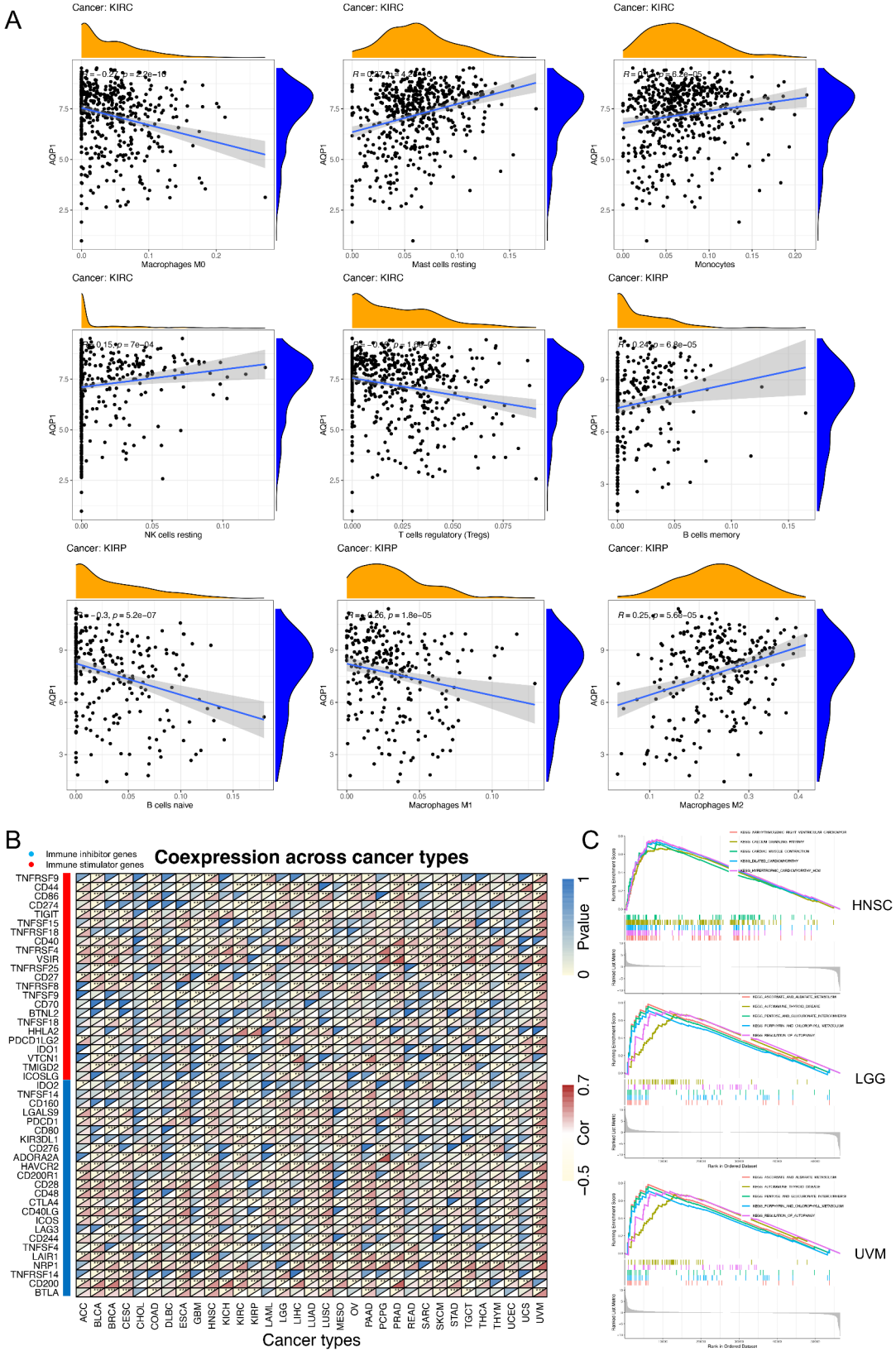

Fig. 6 (See legend on next page.)

(See figure on previous page.)

Fig. 6 AQP1 expression correlated with tumor immunity and enrichment pathways. (**A**) The correlation between AQP1 expression and different types of immune cell infiltration of KIRC and KIRP. (**B**) The heatmap of AQP1 expression and IRGs correlation. The Y-axis displayed the analyzed immune genes, with blue indicating inhibitory genes and red indicating promotive genes. The X-axis represented the cancer type. Asterisks denoted statistical significance. The detailed correlation values were shown in triangles, with blue indicating negative values and red indicating positive values. (**C**) The plots showed the enrichment score in the top 5 ranked list of pathways influenced by AQP1 expression. The top portion of the plot displayed the name of pathways. The middle portion marked the position of genes within each set across the ranked list, while the bottom plot provides the ranked list metric, illustrating the distribution of the metric scores across all ranked genes. *IRGs*, *immune related genes*

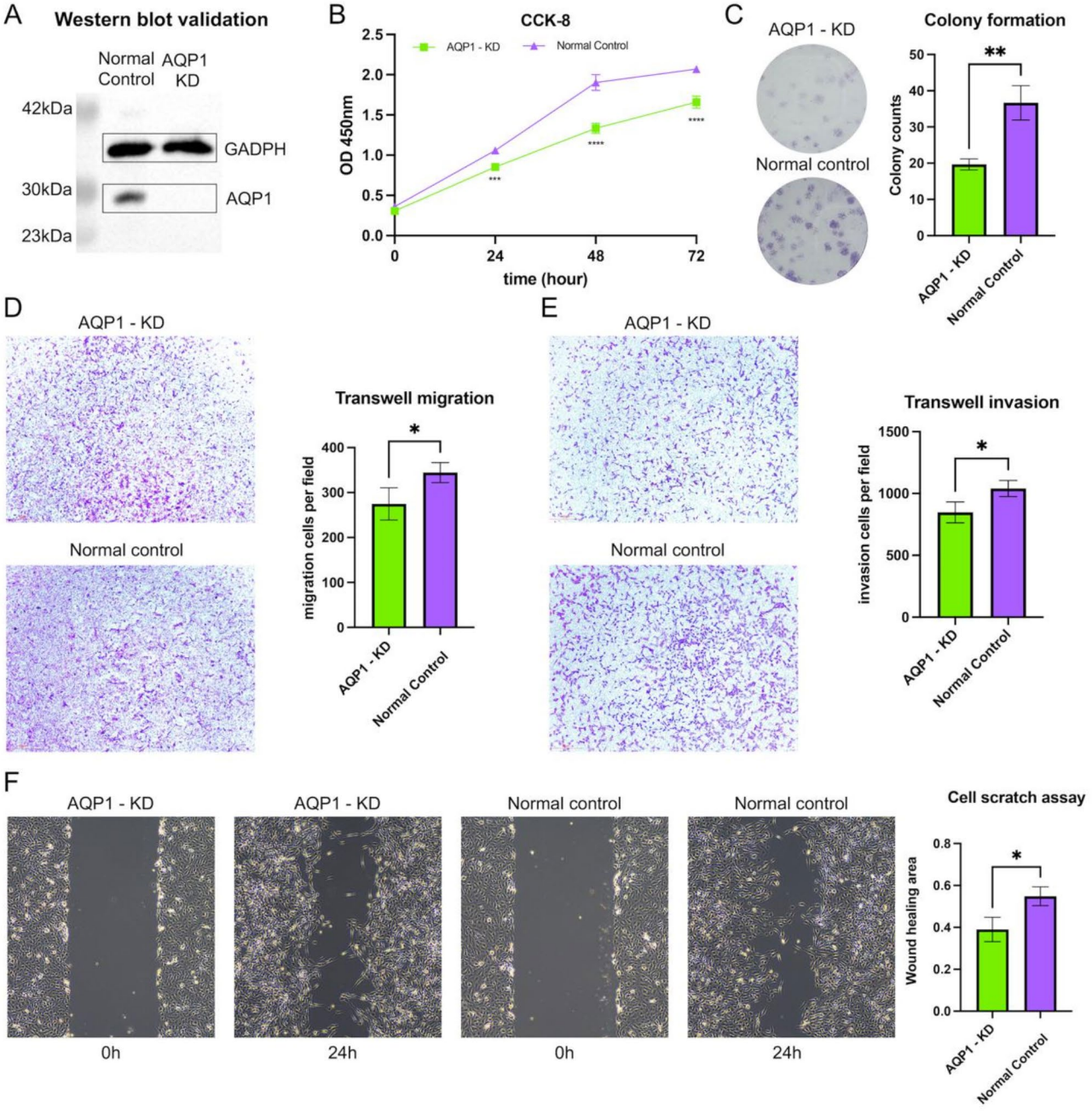

Fig. 7 Knockdown of AQP1 in 786-O cells suppressed cell proliferation, migration and invasion. (**A**) WB validated the stable knockdown of AQP1 in 786-O cells. (**B**) The CCK-8 assay demonstrated reduced cell proliferation in AQP1 knockdown cells. (**C**) The colony formation assay revealed that AQP1 knockdown cells formed less colonies than normal controls. (**D**) The transwell migration assay showed that knockdown of AQP1 suppressed cell migration. (**E**) The transwell invasion assay showed that AQP1 knockdown cells inhibited cell invasion. (**F**) The cell scratch assay revealed that knockdown of AQP1 suppressed wound healing. *WB*, *western blot; CCK-8*, *Cell counting kit-8*

the results in AQP1 expression as a favorable biomarker in renal cancer. Similarly, AQP1 potentially played a similar role in HNSC and SARC. In conclusion, AQP1 was important in the molecular mechanisms of cancers, underlying its potential as an important biomarker in cancer prognosis and treatment.

Limitations of our study

Despite the comprehensive findings of our analysis, certain limitations existed. Firstly, our clinical cohort consisted solely of patients from Xinhua Hospital, and our model was not validated by other centers. Secondly, the pan-cancer data utilized in our research was sourced from online databases, predominantly derived from Western populations. These results may not be broadly applicable to different populations. Lastly, while our study identified AQP1 as a potential biomarker in a pan-cancer context and revealed biological functions of AQP1 in renal cancer cells, the molecular mechanisms of AQP1 required further experimental validation.

Conclusion

Our study revealed that AQP1 has lower expression in tumor tissues compared to normal tissues. Moreover, AQP1 was an independent favorable factor for both OS (HR = 0.32, 95% CI = 0.11–0.9, $P = 0.0308$) and PFS (HR = 0.38, 95% CI = 0.17–0.82, $P = 0.0138$) in RCC patients. Furthermore, in pan-cancer analysis, AQP1 expression was also found to be a potent prognostic biomarker in other malignancies including HNSC, LGG, SARC and UVM. We constructed the ceRNAs and PPI networks, and predicted drug sensitivities related to AQP1. Moreover, the immunity correlation of AQP1 was highly context-dependent, varying significantly with the type of cancer and the immune cell subset involved. AQP1 expression was also related to cell adhesion molecules pathway enrichment in most cancers. Lastly, knockdown of AQP1 inhibited cell proliferation, migration and invasion in 786-O cells,.

Abbreviations

AQPs	aquaporins
KIRC	kidney renal clear cell carcinoma
KIRP	kidney renal papillary cell carcinoma
BRCA	breast cancer
COAD	colon adenocarcinoma
EMT	epithelial-mesenchymal transition
IHC	immunohistochemical
ceRNAs	competing endogenous RNAs
TMA	tissue microarrays
K-M	Kaplan-Meier
OS	overall survival
PFS	progression-free survival
TCGA	The Cancer Genome Atlas
HPA	Human Protein Atlas
ESTIMATE	Estimation of Stromal and Immune Cells in Malignant Tumors Using Expression Data
TMB	tumor mutation burden
MSI	microsatellite instability
miRNA	microRNA
GSCA	Gene Set Cancer Analysis
CIBERSORT	Cell-type Identification By Estimating Relative Subsets Of RNA Transcripts
SCDVA	Single-cell RNA-seq Data Visualization and Analysis
TIMER	Tumor Immune Estimation Resource
TIDE	Tumor Immune Dysfunction and Exclusion
DFS	disease-free survival
DSS	disease-specific survival
lncRNAs	long non-coding RNAs
TIME	tumor immune microenvironment
GSEA	gene set enrichment analysis
HNSC	head and neck squamous cell carcinoma
KICH	kidney chromophobe renal cell carcinoma
LUAD	lung adenocarcinoma
LUSC	lung squamous cell carcinoma
PRAD	prostate adenocarcinoma
READ	rectum adenocarcinoma
SARC	sarcoma
UCEC	uterine corpus endometrial carcinoma
CHOL	cholangiocarcinoma
GBM	glioblastoma multiforme
THCA	thyroid carcinoma
MESO	mesothelioma
LGG	low grade glioma
UVM	uveal melanoma
LIHC	liver hepatocellular carcinoma
STAD	stomach adenocarcinoma
Her2	human epidermal growth factor receptor 2
SKCM	skin cutaneous melanoma
PAAD	pancreatic adenocarcinoma
LUSC	lung squamous cell carcinoma
HNSC	head and neck squamous cell carcinoma
DLBC	diffuse large B-cell lymphoma
CNA	Copy Number Alteration
CNV	Copy Number Variant
BLCA	bladder urothelial carcinoma
LGG	brain lower grade glioma
KIRP	kidney renal papillary cell carcinoma
THYM	thymoma; LUAD, lung adenocarcinoma
LIHC	liver hepatocellular carcinoma
THCA	thyroid carcinoma
PCPG	pheochromocytoma and paraganglioma
READ	rectum adenocarcinoma
PRAD	prostate adenocarcinoma
CESC	cervical squamous cell carcinoma and endocervical adenocarcinoma
SARC	sarcoma
ESCA	esophagus carcinoma
CTLs	cytotoxic T lymphocytes
IRGs	immune-related genes
CAMs	cell adhesion molecules

Supplementary Information

The online version contains supplementary material available at https://doi.org/10.1186/s40246-025-00726-9 .

Supplementary Material 1

Acknowledgements

We thank TCGA database, STRING database, HPA database, cBioportal database, DIANA-microT database, miRWalk database, miRDB database, miRcode database, starbase, CellMiner database, GSEA database, SCDVA database, ScRNA-seq Data Portal for T cell in Pan-Cancer database, TIMER 2.0 database, and TIDE database for allowing us to use their data.

Author contributions

Y.L., D.L., Y.Y., K.D., and X.P. designed the conception of the reseachK.D. and X.P. collected and aseembled the data.Y.L., D.L., Y.Y., J.C., J.L., J.C., Z.B. and B.L. analyzed and interpretated the data.Y.L., D.L., Y.Y., J.C., B.L. writed the

manscript.K.D. and X.P. revised the manuscript.Y.L., D.L., Y.Y., J.C., B.L., K.D., X.P. finally approved the manuscript.

Funding
This work was sponsored by the National Natural Science Foundation of China (No. 82072806); Shanghai Rising-Star Program (23QC1401400); Bole project of Shanghai Jiao Tong University. The funders had no role in study design, data collection and analysis, decision to publish, or preparation of the manuscript.

Data availability
The datasets generated and/or analyzed during the current study are available on the The Cancer Genome Atlas (TCGA) database (https://cancergenome.nih.gov/), the Search Tools for the Retrieval of Interacting Genes/Proteins (STRING) database (https://string-db.org/), Human Protein Atlas (HPA) database (https://www.proteinatlas.org/), cBioportal database (https://www.cbioportal.org/) DIANA-microT database(https://dianalab.e-ce.uth.gr/microt_webserver/#/), miRWalk database (https://mirwalk.umm.uni-heidelberg.de/), miRDB database (https://mirdb.org/), and miRcode database (http://www.mircode.org), starbase (http://starbase.sysu.edu.cn/), CellMiner database (https://discover.nci.nih.gov/cellminer/home.do), the Gene Set Cancer Analysis (GSCA) websites (http://bioinfo.life.hust.edu.cn/GSCA), ScRNA-seq Data Visualization and Analysis (SCDVA) database (http://panmyeloid.cancer-pku.cn/, http://pan-nk.cancer-pku.cn/), ScRNA-seq Data Portal for T cell in Pan-Cancer database (http://cancer-pku.cn:3838/PanC_T/), Tumor Immune Estimation Resource (TIMER) 2.0 database (http://timer.cistrome.org/) and Tumor Immune Dysfunction and Exclusion (TIDE) database.

Declarations

Ethics approval and consent to participate
The study was approved by the Ethics Committee of Xinhua Hospital Affiliated to Shanghai Jiao Tong University School of Medicine (XHEC-C-2021-145-1). We confirm that our clinical cohort study adheres fully to the principles outlined in the Declaration of Helsinki. All authors confirmed that all methods were carried out in accordance with relevant guidelines and regulations.

Consent for publication
For our Xinhua cohort, consent was obtained from the participants (or from parents or legal guardians for children under 16. Any personally identifiable biomedical, clinical, or biometric data included in the manuscript was informed consent from the subjects.

Competing interests
The authors declare no competing interests.

Received: 22 December 2024 / Accepted: 12 February 2025
Published online: 23 February 2025

References

1. Login FH, Nejsum LN. Aquaporin water channels: roles beyond renal water handling. Nat Rev Nephrol. 2023;19(9):604–18.
2. Zhang J, Li S, Deng F, Baikeli B, Yu W, Liu G. Distribution of aquaporins and sodium transporters in the gastrointestinal tract of a desert hare, Lepus yarkandensis. Sci Rep. 2019;9(1):16639.
3. Hua Y, Ying X, Qian Y, Liu H, Lan Y, Xie A et al. Physiological and pathological impact of AQP1 knockout in mice. Biosci Rep. 2019;39(5).
4. Borgnia M, Nielsen S, Engel A, Agre P. Cellular and molecular biology of the aquaporin water channels. Annu Rev Biochem. 1999;68:425–58.
5. Yadav E, Yadav N, Hus A, Yadav JS. Aquaporins in lung health and disease: emerging roles, regulation, and clinical implications. Respir Med. 2020;174:106193.
6. Aslesh T, Al-Aghbari A, Yokota T. Assessing the role of Aquaporin 4 in skeletal muscle function. Int J Mol Sci. 2023;24(2).
7. Tie L, Wang D, Shi Y, Li X. Aquaporins in Cardiovascular System. Adv Exp Med Biol. 2017;969:105–13.
8. Ye Y, Ran J, Yang B, Mei Z. Aquaporins in Digestive System. Adv Exp Med Biol. 2023;1398:145–54.
9. Morrissey JJ, Kharasch ED. The specificity of urinary aquaporin 1 and perilipin 2 to screen for renal cell carcinoma. J Urol. 2013;189(5):1913–20.
10. Huang Y, Murakami T, Sano F, Kondo K, Nakaigawa N, Kishida T, et al. Expression of aquaporin 1 in primary renal tumors: a prognostic indicator for clear-cell renal cell carcinoma. Eur Urol. 2009;56(4):690–8.
11. Song JB, Morrissey JJ, Mobley JM, Figenshau KG, Vetter JM, Bhayani SB, et al. Urinary aquaporin 1 and perilipin 2: can these novel markers accurately characterize small renal masses and help guide patient management? Int J Urol. 2019;26(2):260–5.
12. Yun S, Sun PL, Jin Y, Kim H, Park E, Park SY, et al. Aquaporin 1 is an independent marker of poor prognosis in Lung Adenocarcinoma. J Pathol Transl Med. 2016;50(4):251–7.
13. Zhu L, Ma N, Wang B, Wang L, Zhou C, Yan Y, et al. Significant prognostic values of aquaporin mRNA expression in breast cancer. Cancer Manag Res. 2019;11:1503–15.
14. Abdelrahman AE, Ibrahim DA, El-Azony A, Alnagar AA, Ibrahim A. ERCC1, PARP-1, and AQP1 as predictive biomarkers in colon cancer patients receiving adjuvant chemotherapy. Cancer Biomark. 2020;27(2):251–64.
15. Pini N, Huo Z, Kym U, Holland-Cunz S, Gros SJ. AQP1-Driven Migration is Independent of other known adverse factors but requires a hypoxic undifferentiated cell Profile in Neuroblastoma. Child (Basel). 2021;8(1).
16. Galán-Cobo A, Ramírez-Lorca R, Toledo-Aral JJ, Echevarría M. Aquaporin-1 plays important role in proliferation by affecting cell cycle progression. J Cell Physiol. 2016;231(1):243–56.
17. Li J, Zhang M, Mao Y, Li Y, Zhang X, Peng X, et al. The potential role of aquaporin 1 on aristolochic acid I induced epithelial mesenchymal transition on HK-2 cells. J Cell Physiol. 2018;233(6):4919–25.
18. Liu Y, Yao Y, Yang X, Wei M, Lu B, Dong K, et al. Lymphocyte activation gene 3 served as a potential prognostic and immunological biomarker across various cancer types: a clinical and pan-cancer analysis. Clin Transl Immunol. 2024;13(10):e70009.
19. Tomczak K, Czerwińska P, Wiznerowicz M. The Cancer Genome Atlas (TCGA): an immeasurable source of knowledge. Contemp Oncol (Pozn). 2015;19(1a):A68–77.
20. Tastsoglou S, Alexiou A, Karagkouni D, Skoufos G, Zacharopoulou E, Hatzigeorgiou AG. DIANA-microT 2023: including predicted targets of virally encoded miRNAs. Nucleic Acids Res. 2023;51(W1):W148–53.
21. Sticht C, De La Torre C, Parveen A, Gretz N. miRWalk: an online resource for prediction of microRNA binding sites. PLoS ONE. 2018;13(10):e0206239.
22. Chen Y, Wang X. miRDB: an online database for prediction of functional microRNA targets. Nucleic Acids Res. 2020;48(D1):D127–31.
23. Li JH, Liu S, Zhou H, Qu LH, Yang JH. starBase v2.0: decoding miRNA-ceRNA, miRNA-ncRNA and protein-RNA interaction networks from large-scale CLIP-Seq data. Nucleic Acids Res. 2014;42(Database issue):D92–7.
24. Reinhold WC, Sunshine M, Liu H, Varma S, Kohn KW, Morris J, et al. CellMiner: a web-based suite of genomic and pharmacologic tools to explore transcript and drug patterns in the NCI-60 cell line set. Cancer Res. 2012;72(14):3499–511.
25. Liu CJ, Hu FF, Xie GY, Miao YR, Li XW, Zeng Y et al. GSCA: an integrated platform for gene set cancer analysis at genomic, pharmacogenomic and immunogenomic levels. Brief Bioinform. 2023;24(1).
26. Tang F, Li J, Qi L, Liu D, Bo Y, Qin S, et al. A pan-cancer single-cell panorama of human natural killer cells. Cell. 2023;186(19):4235–e5120.
27. Cheng S, Li Z, Gao R, Xing B, Gao Y, Yang Y, et al. A pan-cancer single-cell transcriptional atlas of tumor infiltrating myeloid cells. Cell. 2021;184(3):792–e80923.
28. Zheng L, Qin S, Si W, Wang A, Xing B, Gao R, et al. Pan-cancer single-cell landscape of tumor-infiltrating T cells. Science. 2021;374(6574):abe6474.
29. Yang Y, Chen X, Pan J, Ning H, Zhang Y, Bo Y, et al. Pan-cancer single-cell dissection reveals phenotypically distinct B cell subtypes. Cell. 2024;187(17):4790–e81122.
30. Gao Y, Li J, Cheng W, Diao T, Liu H, Bo Y et al. Cross-tissue human fibroblast atlas reveals myofibroblast subtypes with distinct roles in immune modulation. Cancer Cell. 2024;42(10):1764–1783.e10.
31. Yoshihara K, Shahmoradgoli M, Martínez E, Vegesna R, Kim H, Torres-Garcia W, et al. Inferring tumour purity and stromal and immune cell admixture from expression data. Nat Commun. 2013;4:2612.
32. Morris GM, Huey R, Lindstrom W, Sanner MF, Belew RK, Goodsell DS, et al. AutoDock4 and AutoDockTools4: automated docking with selective receptor flexibility. J Comput Chem. 2009;30(16):2785–91.
33. Trott O, Olson AJ. AutoDock Vina: improving the speed and accuracy of docking with a new scoring function, efficient optimization, and multithreading. J Comput Chem. 2010;31(2):455–61.

34. Li J, Wu C, Hu H, Qin G, Wu X, Bai F, et al. Remodeling of the immune and stromal cell compartment by PD-1 blockade in mismatch repair-deficient colorectal cancer. Cancer Cell. 2023;41(6):1152–e697.
35. Boulch M, Cazaux M, Loe-Mie Y, Thibaut R, Corre B, Lemaître F et al. A cross-talk between CAR T cell subsets and the tumor microenvironment is essential for sustained cytotoxic activity. Sci Immunol. 2021;6(57).
36. Li M, He M, Xu F, Guan Y, Tian J, Wan Z, et al. Abnormal expression and the significant prognostic value of aquaporins in clear cell renal cell carcinoma. PLoS ONE. 2022;17(3):e0264553.
37. Ticozzi-Valerio D, Raimondo F, Pitto M, Rocco F, Bosari S, Perego R, et al. Differential expression of AQP1 in microdomain-enriched membranes of renal cell carcinoma. Proteom Clin Appl. 2007;1(6):588–97.
38. Devuyst O, Burrow CR, Smith BL, Agre P, Knepper MA, Wilson PD. Expression of aquaporins-1 and– 2 during nephrogenesis and in autosomal dominant polycystic kidney disease. Am J Physiol. 1996;271(1 Pt 2):F169–83.
39. Hoque MO, Soria JC, Woo J, Lee T, Lee J, Jang SJ, et al. Aquaporin 1 is overexpressed in lung cancer and stimulates NIH-3T3 cell proliferation and anchorage-independent growth. Am J Pathol. 2006;168(4):1345–53.
40. Aishima S, Kuroda Y, Nishihara Y, Taguchi K, Iguchi T, Taketomi A, et al. Down-regulation of aquaporin-1 in intrahepatic cholangiocarcinoma is related to tumor progression and mucin expression. Hum Pathol. 2007;38(12):1819–25.
41. Xu S, Huang S, Li D, Zou Q, Yuan Y, Yang Z. The expression of Aquaporin-1 and Aquaporin-3 in extrahepatic cholangiocarcinoma and their clinicopathological significance. Am J Med Sci. 2022;364(2):181–91.
42. Oishi M, Munesue S, Harashima A, Nakada M, Yamamoto Y, Hayashi Y. Aquaporin 1 elicits cell motility and coordinates vascular bed formation by down-regulating thrombospondin type-1 domain-containing 7A in glioblastoma. Cancer Med. 2020;9(11):3904–17.
43. Lamarca A, Santos-Laso A, Utpatel K, La Casta A, Stock S, Forner A, et al. Liver metastases of Intrahepatic Cholangiocarcinoma: implications for an updated staging system. Hepatology. 2021;73(6):2311–25.
44. Lin H, Liu C, Hu A, Zhang D, Yang H, Mao Y. Understanding the immunosuppressive microenvironment of glioma: mechanistic insights and clinical perspectives. J Hematol Oncol. 2024;17(1):31.
45. He JL, Yan YZ, Zhang Y, Li JS, Wang F, You Y et al. A machine learning model utilizing delphian lymph node characteristics to predict contralateral central lymph node metastasis in papillary thyroid carcinoma: a prospective multi-center study. Int J Surg. 2024;111(1):360–370
46. Huttenlocher A. Cell polarization mechanisms during directed cell migration. Nat Cell Biol. 2005;7(4):336–7.
47. Guan B, Zhu D, Dong Z, Yang Z. [Expression and distribution of aquaporin 1 in laryngeal carcinoma]. Lin Chuang Er Bi Yan Hou Tou Jing Wai Ke Za Zhi. 2007;21(6):269–72.
48. Lehnerdt GF, Bachmann HS, Adamzik M, Panic A, Köksal E, Weller P, et al. AQP1, AQP5, Bcl-2 and p16 in pharyngeal squamous cell carcinoma. J Laryngol Otol. 2015;129(6):580–6.
49. Pan W, Huang W, Zheng J, Meng Z, Pan X. Construction of a prognosis model of head and neck squamous cell carcinoma pyroptosis and an analysis of immuno-phenotyping based on bioinformatics. Transl Cancer Res. 2024;13(1):299–316.
50. Mendes CB, da Rocha LS, de Carvalho Fraga CA, Ximenes-da-Silva A. Homeostatic status of thyroid hormones and brain water movement as determinant factors in biology of cerebral gliomas: a pilot study using a bioinformatics approach. Front Neurosci. 2024;18:1349421.
51. Liu J, Wu S, Xie X, Wang Z, Lei Q. Identification of potential crucial genes and key pathways in osteosarcoma. Hereditas. 2020;157(1):29.
52. Shimasaki M, Kanazawa Y, Sato K, Tsuchiya H, Ueda Y. Aquaporin-1 and– 5 are involved in the invasion and proliferation of soft tissue sarcomas. Pathol Res Pract. 2018;214(1):80–8.
53. Gong Z, Zhang J, Guo W. Tumor purity as a prognosis and immunotherapy relevant feature in gastric cancer. Cancer Med. 2020;9(23):9052–63.
54. Palmeri M, Mehnert J, Silk AW, Jabbour SK, Ganesan S, Popli P, et al. Real-world application of tumor mutational burden-high (TMB-high) and microsatellite instability (MSI) confirms their utility as immunotherapy biomarkers. ESMO Open. 2022;7(1):100336.
55. Gedaly R, Angulo P, Hundley J, Daily MF, Chen C, Koch A, et al. PI-103 and sorafenib inhibit hepatocellular carcinoma cell proliferation by blocking Ras/Raf/MAPK and PI3K/AKT/mTOR pathways. Anticancer Res. 2010;30(12):4951–8.
56. Kong B, Zhao S, Kang X, Wang B. MicroRNA-133a-3p inhibits cell proliferation, migration and invasion in colorectal cancer by targeting AQP1. Oncol Lett. 2021;22(3):649.
57. Smart JA, Oleksak JE, Hartsough EJ. Cell adhesion molecules in plasticity and metastasis. Mol Cancer Res. 2021;19(1):25–37.
58. Gires O, Pan M, Schinke H, Canis M, Baeuerle PA. Expression and function of epithelial cell adhesion molecule EpCAM: where are we after 40 years? Cancer Metastasis Rev. 2020;39(3):969–87.
59. Hu J, Verkman AS. Increased migration and metastatic potential of tumor cells expressing aquaporin water channels. Faseb j. 2006;20(11):1892–4.
60. Yin Z, Chen W, Yin J, Sun J, Xie Q, Wu M, et al. RIPK1 is a negative mediator in Aquaporin 1-driven triple-negative breast carcinoma progression and metastasis. NPJ Breast Cancer. 2021;7(1):53.
61. Login FH, Jensen HH, Pedersen GA, Koffman JS, Kwon TH, Parsons M, et al. Aquaporins differentially regulate cell-cell adhesion in MDCK cells. Faseb j. 2019;33(6):6980–94.
62. Monzani E, Bazzotti R, Perego C, La Porta CA. AQP1 is not only a water channel: it contributes to cell migration through Lin7/beta-catenin. PLoS ONE. 2009;4(7):e6167.
63. Huo Z, Lomora M, Kym U, Palivan C, Holland-Cunz SG, Gros SJ. AQP1 is Up-Regulated by Hypoxia and leads to increased cell water permeability, motility, and Migration in Neuroblastoma. Front Cell Dev Biol. 2021;9:605272.
64. Saadoun S, Papadopoulos MC, Hara-Chikuma M, Verkman AS. Impairment of angiogenesis and cell migration by targeted aquaporin-1 gene disruption. Nature. 2005;434(7034):786–92.
65. Qin F, Zhang H, Shao Y, Liu X, Yang L, Huang Y, et al. Expression of aquaporin1, a water channel protein, in cytoplasm is negatively correlated with prognosis of breast cancer patients. Oncotarget. 2016;7(7):8143–54.
66. Ji Y, Liao X, Jiang Y, Wei W, Yang H. Aquaporin 1 knockdown inhibits triple-negative breast cancer cell proliferation and invasion in vitro and in vivo. Oncol Lett. 2021;21(6):437.
67. Wang Z, Wang Y, He Y, Zhang N, Chang W, Niu Y. Aquaporin-1 facilitates proliferation and invasion of gastric cancer cells via GRB7-mediated ERK and Ras activation. Anim Cells Syst (Seoul). 2020;24(5):253–9.
68. Vacca A, Frigeri A, Ribatti D, Nicchia GP, Nico B, Ria R, et al. Microvessel overexpression of aquaporin 1 parallels bone marrow angiogenesis in patients with active multiple myeloma. Br J Haematol. 2001;113(2):415–21.
69. Pan H, Sun CC, Zhou CY, Huang HF. Expression of aquaporin-1 in normal, hyperplasic, and carcinomatous endometria. Int J Gynaecol Obstet. 2008;101(3):239–44.
70. Camerino GM, Nicchia GP, Dinardo MM, Ribatti D, Svelto M, Frigeri A. In vivo silencing of aquaporin-1 by RNA interference inhibits angiogenesis in the chick embryo chorioallantoic membrane assay. Cell Mol Biol (Noisy-le-grand). 2006;52(7):51–6.
71. Nielsen S, Frøkiaer J, Marples D, Kwon TH, Agre P, Knepper MA. Aquaporins in the kidney: from molecules to medicine. Physiol Rev. 2002;82(1):205–44.
72. Maunsbach AB, Marples D, Chin E, Ning G, Bondy C, Agre P, et al. Aquaporin-1 water channel expression in human kidney. J Am Soc Nephrol. 1997;8(1):1–14.

Publisher's note